Research Article

He Liu*, Junhua Jiao, You Tian, Jia'ao Liu, Pei Yuan, and Xuehong Wu

Drying kinetics of *Pleurotus eryngii* slices during hot air drying

https://doi.org/10.1515/phys-2022-0029
received March 14, 2022; accepted April 03, 2022

Abstract: Hot air drying is widely adopted to extend the shelf life of *Pleurotus eryngii*, which is an edible fungus with high nutritional value and large market demand. Understanding moisture transfer during hot air drying is essential for both quality improvement and energy-efficient dryer design. In this study, we investigated the drying kinetics of *P. eryngii* slices with different thicknesses (4, 8, and 12 mm) under different hot air temperature levels (40, 50, 60, 70, and 80°C) and a constant air velocity (2 m/s). It is found that the drying rate increases with the increase of the hot air temperature or the decrease of the thickness of *P. eryngii* slices. Only a falling rate period was observed during the hot air drying. We used eight mathematical models to describe the drying kinetics of *P. eryngii* slices and found that the logarithmic model fits the experimental data best. The fitted effective moisture diffusivity of *P. eryngii* slices is in the range of 3.34×10^{-9} to 2.25×10^{-9} m^2/s, and the fitted drying activation energy is 19.30 kJ/mol, agreeing with the results in the literature. Additionally, we noticed that the color of dried *P. eryngii* slices becomes darker with the increase of hot air temperature due to the Maillard browning reaction. This study helps to understand the drying kinetics of *P. eryngii* slices during the hot air drying and guides the drying process optimization.

Keywords: *Pleurotus eryngii*, hot air drying, heat transfer, moisture transfer

*** Corresponding author: He Liu,** Department of New Energy Science and Engineering, School of Energy and Power Engineering, Zhengzhou University of Light Industry, Zhengzhou 450002, China, e-mail: liuhe@zzuli.edu.cn
Junhua Jiao, You Tian, Jia'ao Liu, Pei Yuan: Department of New Energy Science and Engineering, School of Energy and Power Engineering, Zhengzhou University of Light Industry, Zhengzhou 450002, China
Xuehong Wu: Department of Energy and Power Engineering, Zhengzhou University of Light Industry, Zhengzhou 450002, China

1 Introduction

Pleurotus eryngii is a kind of edible fungus which has high nutritional value, thick flesh, and large market demand [1]. However, it is challenging to store fresh *P. eryngii* with high moisture content at room temperature due to its relatively high metabolic activity. Therefore, fresh *P. eryngii* needs to be consumed or processed immediately after harvest. Drying is an important method to remove the water inside *P. eryngii*. Generally, the moisture content of fresh *P. eryngii* can be effectively reduced from up to 90% (wet basis) to a safe moisture level of 13% (wet basis), which simultaneously reduces their water activity, inhibits microbial growth, and enlarges shelf life [2]. More importantly, drying maintains the nutritional ingredients and flavor of fresh products.

Owing to simplicity and low cost, open sun drying has been adopted to process agricultural products from thousands of years ago. However, it involves drawbacks, including dust and microbial contamination of the dried materials as well as overlong drying time [3], which is not suitable for drying *P. eryngii*. A simple and cost-effective hot air drying, which accelerates the drying process by blowing hot air into the oven or drying room, can overcome the drawbacks of open sun drying and be used for drying *P. eryngii* [4]. During hot air drying, moisture inside of a product first diffuses to its surface and then transfers to the surrounding air under temperature and moisture gradient. Therefore, understanding the effect of ambient conditions (*e.g.*, temperature, humidity) and moisture transport inside the product on the drying process is important to optimize the drying process, improve product quality, design new dryers, and save energy. In early studies on hot air drying, most works focused on product quality, including shrinkage, rehydration, hardness, content, and type of amino acid. With the gradual recognition of the importance of drying kinetics, a number of recent works centered on the moisture diffusion of various vegetables and fruits, such as parsley leaves [5], golden apples [6], banana [7], berberis [8], and tomato [9]. However, few are known about the drying kinetics of *P. eryngii*.

In this study, we aim to experimentally investigate the drying kinetics of *P. eryngii* slices during the hot air drying process. The effects of hot air temperature and slice thickness on drying kinetics were studied. The effective moisture diffusivity and drying activation energy were obtained based on the empirical mathematical models. Besides, the quality of dried *P. eryngii* slices was assessed according to the color change after drying.

2 Experiment

2.1 Materials

P. eryngii (5–6 cm in diameter and ~150 cm in length) was purchased from a local vegetable market in Zhengzhou, China. The samples with an average initial moisture content of 88–92% (wet basis, g water/g matter) were selected as the raw materials for the drying experiment [10]. Then, the fungi were stored in a refrigerator at a temperature of 4°C. Before drying experiments, the *P. eryngii* was first placed in room temperature (20°C) for about 2 h for thermal equilibrium.

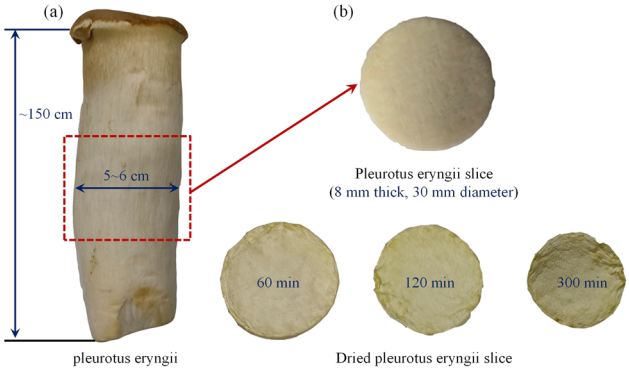

Figure 1: (a) Fresh *P. eryngii* and its slices and (b) before and after drying.

2.2 Experimental apparatus

A temperature-controlled and wind velocity-controlled electric blast oven (Model DHG-9070, Shanghai Yiheng Scientific Instrument Co., Ltd, China) was used to perform hot air drying. The initial mass and the mass during drying were determined with precise digital balance with the accuracy of 0.001 g (Model ES500, Shanghai Yueping Scientific Instrument Co., Ltd, China).

2.3 Experimental procedure

Before each experiment, the *P. eryngii* was washed quickly with distilled water and wiped with paper towels. The same sections of fungus were manually cut into thin cylindrical slices with a diameter of 30 mm and various thicknesses (4, 8, and 12 mm, Figure 1). Since the skin of the *P. eryngii* in contact with distilled water would be removed, the effect of the cleaning process on the moisture content of the fungus slices could be neglected. Then, the slices were placed in the drying chamber with a constant temperature (40, 50, 60, 70, and 80°C, respectively), a relative humidity of 20%, and an air velocity of 2 m/s (Figure 2). To avoid the influence of temperature rise process, the oven was kept for at least 20 min at the set point. The mass of samples was measured and recorded every 15 min. The weighing time is controlled

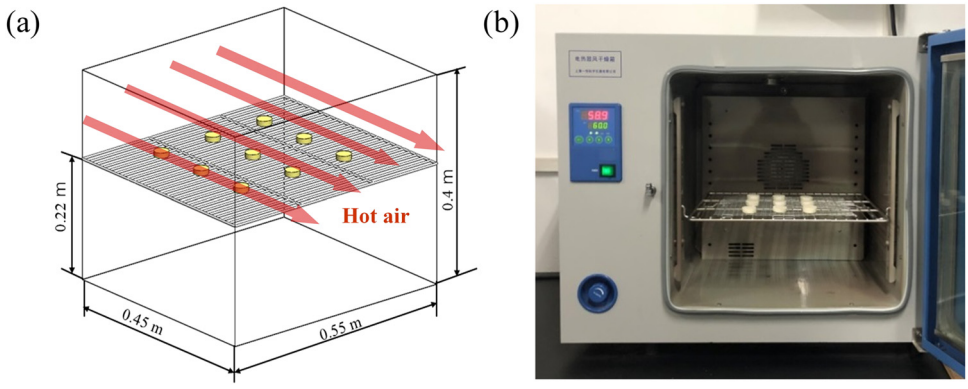

Figure 2: Hot air drying process: (a) schematic of the hot air drying process and (b) drying chamber.

Table 1: Design of the drying experiments of *P. eryngii* slices

Group	Number	Experimental parameters	Value	Constant parameters
1	1	Hot air	40	Sample
	2	temperature (°C)	50	thickness 8 mm
	3		60	
	4		70	
	5		80	
2	6	Sample	4	Hot air
	7	thickness (mm)	8	temperature 70°C
	8		12	

within 20 s to ensure that the weight loss of the sample before and after weighing is less than 0.01 g. The experiments were stopped when the moisture content of the samples reached the equilibrium moisture content (10–13%, wet basis). Each drying process was repeated five times, and the average value was used for the subsequent analysis (Table 1).

3 Drying kinetics

3.1 Drying models

Eight thin-layer mathematical drying models were chosen to fit the variation of dimensionless moisture ratio (MR) as a function of time (t) during the drying process of *P. eryngii* slices (Table 2), where the dimensionless MR of *P. eryngii* slices can be calculated by ref. [19],

$$\mathrm{MR} = \frac{M_t - M_\mathrm{e}}{M_0 - M_\mathrm{e}}, \tag{1}$$

where M_t, M_0, and M_e are the moisture content at time t, initial moisture content, and equilibrium moisture content (g water/g dry matter, dry basis), respectively.

The moisture content is defined as,

$$M_t = \frac{W_t - W_\mathrm{d}}{W_\mathrm{d}}, \tag{2}$$

where W_t and W_d are the mass of samples at time t and the mass of dried samples (g), respectively. The drying rate of *P. eryngii* slices can be evaluated by ref. [20],

$$\mathrm{DR}=\frac{M_{t+\mathrm{d}t} - M_t}{\Delta t}, \tag{3}$$

where DR is the drying rate, Δt is the time interval between two measurements, and $M_{t+\mathrm{d}t}$ is the moisture content at $(t + \mathrm{d}t)$. The effectiveness of the models was evaluated by the correlation coefficient (R^2), the sum of squared error (SSE), and root-mean-square error (RMSE), which are defined by ref. [21],

$$R^2 = 1 - \frac{\sum_{i=1}^{N}(\mathrm{MR}_{\mathrm{exp},i} - \mathrm{MR}_{\mathrm{pre},i})^2}{\sum_{i=1}^{N}(\mathrm{MR}_{\mathrm{exp},i} - \mathrm{MR}_{\mathrm{exp}})^2}, \tag{4}$$

$$\mathrm{SSE} = \sum_{i=1}^{N}(\mathrm{MR}_{\mathrm{exp},i} - \mathrm{MR}_{\mathrm{pre},i})^2, \tag{5}$$

$$\mathrm{RMSE} = \sqrt{\frac{\sum_{i=1}^{N}(\mathrm{MR}_{\mathrm{exp},i} - \mathrm{MR}_{\mathrm{pre},i})^2}{N}}, \tag{6}$$

where $\mathrm{MR}_{\mathrm{exp},i}$ is the experimental MR in the ith test, $\mathrm{MR}_{\mathrm{pre},i}$ is the predicted MR, $\mathrm{MR}_{\mathrm{exp}}$ is the mean experimental MR, and N is the number of drying experiments. According to Eqs. (4)–(6), a lager R^2 and a smaller SSR of RMSE indicate a better model.

3.2 Effective moisture diffusivity

The effective moisture diffusivity can be determined by solving Fick's second diffusion model [3], which states,

$$\frac{\partial \mathrm{MR}}{\partial t} = \nabla^2 \mathrm{MR}. \tag{7}$$

Table 2: Mathematical drying models for thin-layer drying

Number	Model	Expression	References
1	Newton	$\mathrm{MR} = \exp(-kt)$	[11]
2	Page	$\mathrm{MR} = \exp(-kt^n)$	[12]
3	Henderson & Pabis	$\mathrm{MR} = a\exp(-kt)$	[13]
4	Wang & Singh	$\mathrm{MR} = 1 + at + bt^2$	[14]
5	Midilli & others	$\mathrm{MR} = a\exp(-kt) + bt$	[15]
6	Logarithmic	$\mathrm{MR} = a\exp(-kt) + c$	[16]
7	Demir & others	$\mathrm{MR} = a\exp(-kt)^n + b$	[17]
8	Two terms	$\mathrm{MR} = a\exp(-k_1t) + b\exp(-k_2t)$	[18]

For long drying periods, since the diameters of the *P. eryngii* slices are much larger than their thickness, the moisture transport in thickness direction dominates the drying process. Here, the one-dimensional diffusion equation is used to describe the mass transfer process, and Eq. (7) can be simplified as ref. [18],

$$\ln \mathrm{MR} = \ln \frac{8}{\pi^2} - \frac{\pi^2 D_{\mathrm{eff}} t}{L^2}, \tag{8}$$

where D_{eff} is the effective moisture diffusivity and L is the thickness of *P. eryngii* slice.

3.3 Drying activation energy

The relationship between the drying activation energy (E_{a}) and the effective moisture diffusivity can be described by the Arrhenius equation [22].

$$D_{\mathrm{eff}} = D_0 \exp\left(\frac{E_{\mathrm{a}}}{RT}\right), \tag{9}$$

where D_0 is Arrhenius constant, R is gas constant, and T is the absolute temperature.

3.4 Color assessment

A color difference meter was used to investigate the color changes of *P. eryngii* slices during the hot air drying. Since the color difference meter perceives color as Red Green Blue signals, the images were converted into $L^*a^*b^*$ units to ensure the color reproducibility, in which L^* represents lightness/darkness that ranges from 0 to 100, a^* represents redness/greenness that ranges from −120 to 120, and b^* denotes yellowness/blueness that ranges from −120 to 120. The total color difference was calculated by ref. [23],

$$\Delta E = \sqrt{(L^* - L_0{}^*)^2 + (a^* - a_0{}^*)^2 + (b^* - b_0{}^*)^2}, \tag{10}$$

where $L_0{}^*$, $a_0{}^*$, and $b_0{}^*$ represent the color index of fresh *P. eryngii* slices.

Also, the browning index (BI) was calculated by ref. [24],

$$\mathrm{BI} = 100 \times \left(\frac{X - 0.31}{0.17}\right), \tag{11}$$

where

$$X = \frac{(a^* + 1.75L^*)}{(5.645L^* + a^* - 3.012b^*)}.$$

4 Results and discussion

4.1 Drying kinetics of *P. eryngii* slice

4.1.1 Effect of hot air temperature

Figure 3 shows the hot air drying kinetics of *P. eryngii* slice with a thickness of 8 mm at the temperature of 40–80°C and an air velocity of 2 m/s. It is observed that the moisture content of the fungus slices decreases fast with the increase of hot air temperature (Figure 3(a)), resulting in a decreased drying time. As shown in Figure 3(b), it took 250, 210, 160, 140, and 130 min to dry the slices to the equilibrium moisture content at the temperature of 40, 50, 60, 70, and 80°C respectively. This is because the higher temperature gradient between the *P. eryngii* slices and the surrounding environment (hot air) accelerates the evaporation and movement of moisture inside the fungus slices during the hot air drying. Our results are consistent with the reported trends in literature [3,22,25]. Additionally, when the hot air temperature increases from 50 to 60°C, we noticed that the drying time drops sharply, reducing by 85 min. Figure 3(c) shows the drying rate as a function of moisture content. Interestingly, we only observed a falling rate drying period during the entire drying process, and no constant rate drying period was observed. The reason is that the large oven size, compared with the fungus slice, makes the moisture inside and permeating in the drying chamber the slice can be taken away by the hot air in time during the drying process. Therefore, there is no saturated steam around the slice surface. As the drying process progresses, the temperature and moisture gradients between the *P. eryngii* slices and the surrounding hot air decrease gradually. Thus, the drying rate of the slices decreases as moisture content reduces after the initial stage of heating up (Figure 3(c)). Figure 3(d) shows the average drying rate of the slices under different temperatures. It is obvious that the average drying rate increases as the temperature increases because of the larger temperature gradients between the *P. eryngii* slices and the surrounding hot air.

4.1.2 Effect of sample thickness

Figure 4 depicts the drying kinetics of *P. eryngii* slices with different thicknesses (4, 8, and 12 mm) at the hot air temperature of 70°C and an air velocity of 2.0 m/s.

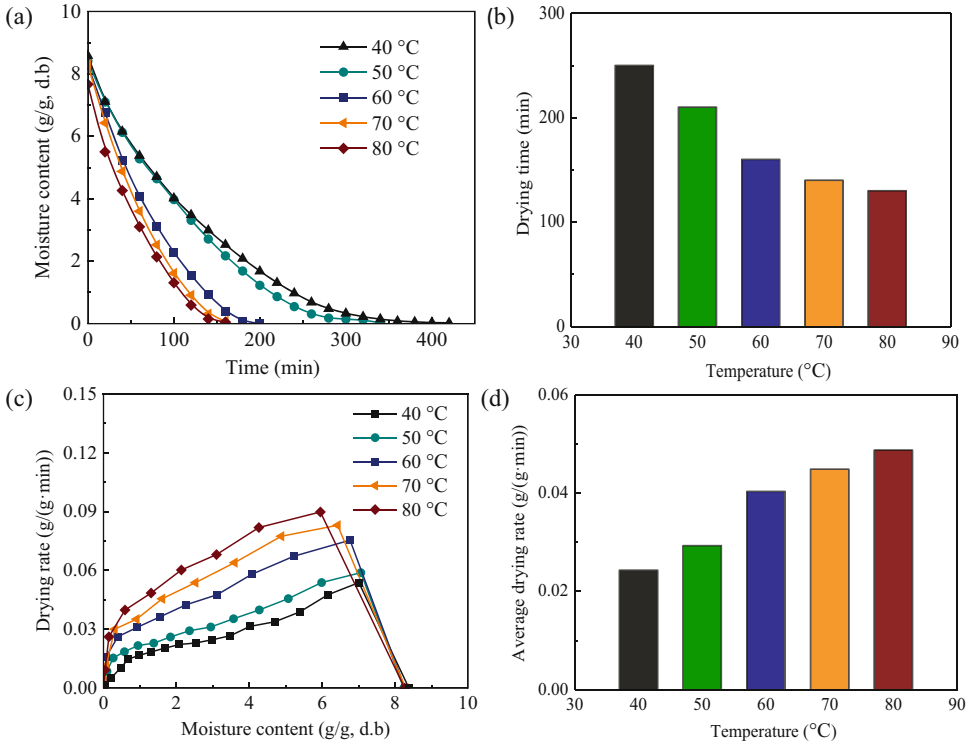

Figure 3: Drying kinetics of *P. eryngii* slices with a thickness of 8 mm and a diameter of 30 mm at different hot air temperatures and an air velocity of 2 m/s. (a) The variation of the moisture content of the slices as a function of time. (b) Comparison of drying time of the slices under various temperatures. (c) The variation of the drying rate of the slices as a function of moisture content. (d) Comparison of drying rate of the slices at various temperatures.

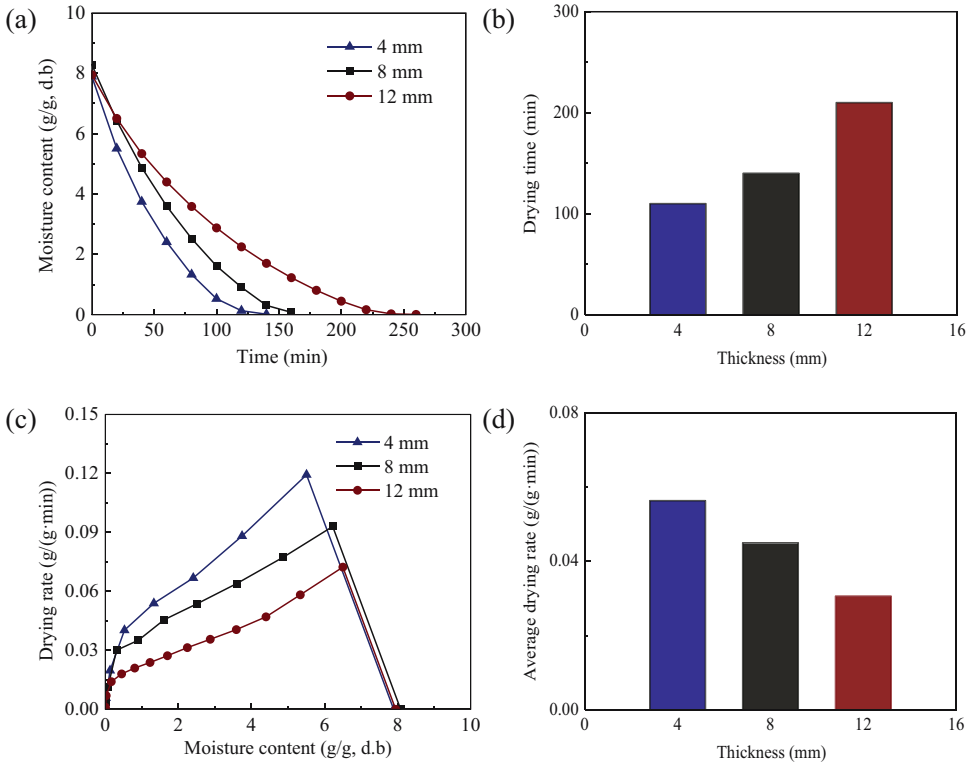

Figure 4: Drying kinetics of *P. eryngii* slices with a diameter of 30 mm and a thickness of 4–12 mm at a hot air temperature of 70°C and an air velocity of 2 m/s. (a) The variation of the moisture content of the slices as a function of time. (b) Comparison of drying time of the slices under various sample thicknesses. (c) The variation of the drying rate of the slices as a function of moisture content. (d) Comparison of drying rate of the slices under various sample thicknesses.

It is observed from Figure 4(a) that the drying time of *P. eryngii* slices increases with the increase of sample thickness. For example, the drying time increases from 110 to 220 min when the sample thickness increases from 4 to 12 mm. This is because the moisture migration path inside *P. eryngii* slices increases as the sample thickness increases, and the relative contact area between the sample and the surrounding (hot air) becomes smaller. Figure 4(b) also shows that the duration of the falling rate drying period increases with the increase of sample thickness. Since the drying process mainly occurs inside the sample during the falling rate drying period, the total moisture content and moisture migration path increase with the increase of the sample thickness, leading to the decreased drying rate. The similar variation trend is also found in ref. [22].

4.2 Evaluation of drying models

We adopted eight mathematical models to fit the drying kinetics of *P. eryngii* slices under various temperatures. The fitting results are shown in Table 3. It is found that

Table 3: Fitting parameters of eight mathematical models

Model	T (°C)	Parameters	R^2	SSE	RMSE
Newton	40	$k = 0.00830$	0.9889	0.0211	0.0317
	50	$k = 0.00879$	0.9805	0.0330	0.0441
	60	$k = 0.01348$	0.9775	0.0261	0.0510
	70	$k = 0.01565$	0.9791	0.0200	0.0500
	80	$k = 0.01705$	0.9821	0.0168	0.0459
Page	40	$k = 0.00439$, $n = 1.127$	0.9900	0.0211	0.0267
	50	$k = 0.00313$, $n = 1.218$	0.9922	0.0094	0.0250
	60	$k = 0.00354$, $n = 1.299$	0.9947	0.0061	0.0261
	70	$k = 0.00445$, $n = 1.292$	0.9950	0.0047	0.0260
	80	$k = 0.00696$, $n = 1.210$	0.9908	0.0087	0.0352
Henderson & Pabis	40	$k = 0.00856$, $a = 1.032$	0.9852	0.0200	0.0324
	50	$k = 0.00993$, $a = 1.092$	0.9850	0.0179	0.0346
	60	$k = 0.01436$, $a = 1.070$	0.9805	0.0226	0.0476
	70	$k = 0.01639$, $a = 1.050$	0.9815	0.0176	0.0470
	80	$k = 0.01744$, $a = 1.024$	0.9830	0.0160	0.0479
Wang & Singh	40	$a = -0.00576$, $b = 8.317 \times 10^{-6}$	0.9852	0.0205	0.0325
	50	$a = -0.00653$, $b = 1.079 \times 10^{-5}$	0.9996	0.0047	0.0177
	60	$a = -0.00968$, $b = 2.342 \times 10^{-5}$	0.9993	0.0008	0.0093
	70	$a = -0.01134$, $b = 3.222 \times 10^{-5}$	0.9960	0.0004	0.0071
	80	$a = -0.01226$, $b = 3.794 \times 10^{-5}$	0.9962	0.0036	0.0227
Midilli & others	40	$a = 0.989$, $k = 0.00732$, $b = -0.00017$	0.9972	0.0053	0.0168
	50	$a = 1.002$, $k = 0.00733$, $b = -0.00033$	0.9964	0.0061	0.0201
	60	$a = 1.013$, $k = 0.01076$, $b = -0.00072$	0.9985	0.0017	0.0147
	70	$a = 1.006$, $k = 0.01211$, $b = -0.00096$	0.9991	0.0008	0.0118
	80	$a = 0.993$, $k = 0.01358$, $b = -0.00080$	0.9977	0.0021	0.0189
Logarithmic	40	$a = 1.071$, $k = 0.00672$, $c = -0.08657$	0.9976	0.0046	0.0155
	50	$a = 1.155$, $k = 0.006439$, $c = -0.15640$	0.9970	0.0051	0.0184
	60	$a = 1.230$, $k = 0.00917$, $c = -0.21980$	0.9989	0.0013	0.0127
	70	$a = 1.259$, $k = 0.01017$, $c = -0.25450$	0.9994	0.0006	0.0098
	80	$a = 1.186$, $k = 0.01172$, $c = -0.19540$	0.9979	0.0020	0.0183
Demir and others	40	$a = 0.831$, $b = 0.055$, $k = 1.676$, $n = 0.00509$	0.9459	0.1025	0.0755
	50	$a = 0.814$, $b = 0.097$, $k = 0.703$, $n = 0.01448$	0.9163	0.1421	0.1007
	60	$a = 0.841$, $b = 0.092$, $k = 0.007$, $n = 2.07300$	0.9262	0.0856	0.1106
	70	$a = 0.958$, $b = 0.032$, $k = 0.014$, $n = 1.19200$	0.9694	0.0292	0.0765
	80	$a = 0.986$, $b = -0.094$, $k = 0.233$, $n = 0.10360$	0.9979	0.0020	0.0201
Two terms	40	$a = 1.032$, $k_1 = 0.0086$, $b = -0.0323$, $k_2 = 1.066$	0.9895	0.0200	0.0333
	50	$a = 1.082$, $k_1 = 0.0095$, $b = -0.0824$, $k_2 = 1.681$	0.9844	0.0264	0.0434
	60	$a = 1.159$, $k_1 = 0.0155$, $b = -0.1590$, $k_2 = 1.189$	0.9878	0.0142	0.0450
	70	$a = 1.159$, $k_1 = 0.0180$, $b = -0.1589$, $k_2 = 1.152$	0.9884	0.0111	0.0471
	80	$a = 1.098$, $k_1 = 0.0186$, $b = -0.0979$, $k_2 = 0.999$	0.9855	0.0137	0.0524

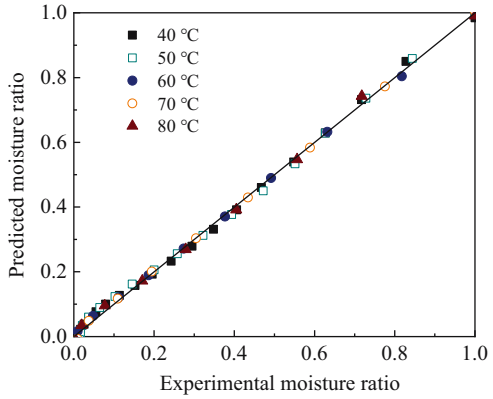

Figure 5: Comparison of MRs of *P. eryngii* slices between the experimental measurements and predicted results from the logarithmic model.

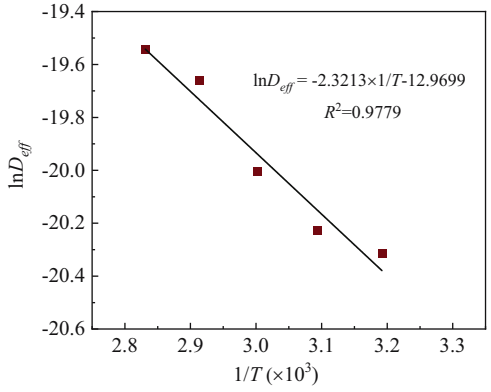

Figure 6: Arrhenius-type relationship between the effective moisture diffusivity and the absolute temperature.

the logarithmic model fit the drying kinetics of the slices best since it results in the highest value of R^2 and the lowest values of SSE and RMSE. The values of R^2, SSE, and RMSE are in the range of 0.9970–0.9994, 0.0006–0.0051, 0.0098–0.0184, respectively. Our results are similar to the drying behavior of thin-layer mushroom slices in literature [26]. Figure 5 shows the comparison of the experimental data and the predicted results from the logarithmic model. The results show that the empirical mathematical model can describe the experimental results well, which provides good results for the engineering application of the food industry [27].

4.3 Effective moisture diffusivity and drying activation energy

The effective moisture diffusivities of *P. eryngii* slices listed in Table 4 were fitted on the basis of Eq. (8). The obtained effective moisture diffusivities of the slices range from to 3.40×10^{-9} m^2/s, agreeing with the reported values of the most agricultural products including mushrooms (10^{-11} to 10^{-9} m^2/s) [25,26,28]. Meanwhile, the effective moisture diffusivity increases as hot air temperature increases. For example, the effective moisture diffusivity of the slides with a thickness of 8 mm increases from 1.51×10^{-9} to 3.26×10^{-9} m^2/s when the hot air temperature increases from 40 to 80°C. This is because the high air temperature accelerates the migration and diffusion of water molecules, which enhances water molecules vaporization ultimately and increases the effective moisture diffusivity. Additionally, since a large sample thickness prolongs the moisture transport path, weakens the migration of moisture, and reduces the effective moisture diffusivity, we see that the effective moisture diffusivity decreases from 3.40×10^{-9} to 2.25×10^{-9} m^2/s when the sample thickness increases from 4 to 12 mm (hot air temperature is 70°C).

The drying activation energy can be obtained by fitting the variation of effective moisture diffusivity as a function of temperature. According to Eq. (9), the Arrhenius constant and activation energy of the fungus slices are 2.33×10^{-6} m^2/s and 19.30 kJ/mol, respectively (Figure 6). The activation energy value is close to the reported value of oyster mushroom, which is 22.23 kJ/mol [25].

Table 4: Effective moisture diffusivity of *P. eryngii* slices under various drying temperatures

Number	Hot air temperature (°C)	Sample thickness (mm)	ln(MR)	D_{eff} (10^{-9} m^2/s)
1	40	8	$\ln MR = -2.3234 \times 10^{-4}t + 0.6322$	1.51
2	50	8	$\ln MR = -2.5338 \times 10^{-4}t + 0.6051$	1.64
3	60	8	$\ln MR = -3.1588 \times 10^{-4}t + 0.5042$	2.05
4	70	8	$\ln MR = -4.4537 \times 10^{-4}t + 0.5103$	2.89
5	80	8	$\ln MR = -5.0246 \times 10^{-4}t + 0.5777$	3.26
6	70	4	$\ln MR = -2.0959 \times 10^{-3}t + 0.6354$	3.40
7	70	12	$\ln MR = -1.5443 \times 10^{-4}t + 0.5016$	2.25

Table 5: Color change of dried *P. eryngii* slices at different hot air temperatures

Hot air temperature (°C)	L^*	a^*	b^*	ΔE	BI
40	86.48	1.87	8.77	5.40	12.03
50	81.07	2.08	9.98	10.57	14.73
60	75.33	1.96	11.49	16.38	18.11
70	74.70	2.02	11.62	17.02	18.53
80	73.52	2.37	13.14	18.73	21.65

4.4 Color measurement

Color is an important indicator of the apparent quality of food ingredients, and the ideal color of dried products is close to fresh color. The color of fresh *P. eryngii* is (L_0^*, a_0^*, b_0^*) = (90.44, 0.69, 5.28), and the BI of the fresh fungus is 6.43. The color parameters of the dried fungus slices are shown in Table 5. According to ref. [29], the lightness (L^*) decreases with increasing hot air temperature, while the redness (a^*) and yellowness (b^*) increase with increasing temperature due to the Maillard browning reaction. It is seen that the total maximum and minimum color difference (ΔE) increasement was 5.40 and 18.73, respectively, when the hot air temperature is in the range of 40–80°C. Besides, we noticed that ΔE increases dramatically when the hot air temperature increases from 50°C to 60°C. Regarding the BI, which corresponds to a quantification of the brown color resulting from the thermal processing, the fresh *P. eryngii* slices showed the lowest value. And the BI of the dried slices increases from 12.03 to 21.65 when the hot air temperature increases from 40 to 80°C. The above phenomenon can be attributed to the increased drying speed as discussed in Section 4.1.1.

5 Conclusion

In summary, we investigated the hot air drying kinetics and dry quality of *P. eryngii* slices with different thicknesses (4, 8, and 12 mm) at different hot air temperatures (40, 50, 60, 70, and 80°C) and a constant air velocity of 2 m/s. The experimental results show that, during the hot air drying process of the slices, only falling rate period exists and no constant rate period was observed. The drying time can be shorted with the increase of hot air temperature and/or the decrease of sample thickness. The logarithmic model fits the drying kinetics of the fungus best. The effective moisture diffusivities are in the range of 3.40×10^{-9} to 2.25×10^{-9} m^2/s and the activation energy is 19.30 kJ/mol. Besides, the color of the dried slices becomes darker with the increase of hot air temperature and the total color change increased from 5.40 to 18.73 when the temperature increased from 40 to 80°C, indicating the Maillard browning reaction of the slices with the reduction of moisture content during drying. This study helps to understand the drying kinetics of *P. eryngii* slices and may guide the drying process optimization and new dryer equipment design.

Funding information: This study was supported by the National Natural Science Foundation of China (No. 51806200), the Foundation of Key Laboratory of Thermo-Fluid Science and Engineering (Xi'an Jiaotong University), Ministry of Education (No. KLTFSE2020KFJJ03), and Henan Association for Science and Technology (No. 2022HYTP017).

Author contributions: H.L. conceived the idea and designed the experiments. J.J., Y.T., and J.L. conducted the experiments. H.L. wrote the manuscript. All authors participated in the discussion of the research. All authors have accepted responsibility for the entire content of this manuscript and approved its submission.

Conflict of interest: The authors state no conflict of interest.

Data availability statement: All of the data supporting the findings are presented within the article. All other data are available from the corresponding author upon reasonable request.

References

[1] Su D, Lv W, Wang Y, Wang L, Li D. Influence of microwave hot-air flow rolling dry-blanching on microstructure, water migration and quality of *Pleurotus eryngii* during hot-air drying. Food Control. 2020;114:107228.
[2] Torki-Harchegani M, Ghasemi-Varnamkhasti M, Ghanbarian D, Sadeghi M, Tohidi M. Dehydration characteristics and mathematical modelling of lemon slices drying undergoing oven treatment. Heat Mass Transf. 2016;52:281–9.
[3] Demiray E, Tulek Y. Thin-layer drying of tomato (Lycopersicum esculentum Mill. cv. Rio Grande) slices in a convective hot air dryer. Heat Mass Transf. 2012;48:841–7.
[4] Li K, Zhang Y, Wang YF, El-Kolaly W, Gao M, Sun W, et al. Effects of drying variables on the characteristic of the hot air drying for gastrodia elata: Experiments and multi-variable model. Energy. 2021;222:119982.
[5] Akpinar EK, Bicer Y, Cetinkaya F. Modelling of thin layer drying of parsley leaves in a convective dryer and under open sun. J Food Eng. 2006;75:308–15.

[6] Menges HO, Ertekin C. Mathematical modeling of thin layer drying of Golden apples. J Food Eng. 2006;77(1):119–25.
[7] Dandamrongrak R, Young G, Mason R. Evaluation of various pre-treatments for the dehydration of banana and selection of suitable drying models. J Food Eng. 2002;55(2):139–46.
[8] Aghbashlo M, Kianmehr MH, Samimi-Akhijahani H. Influence of drying conditions on the effective moisture diffusivity, energy of activation and energy consumption during the thin-layer drying of berberis fruit (Berberidaceae). Energy Convers Manag. 2008;49(10):2865–71.
[9] Demir K, Sacilik K. Solar drying of Ayaş tomato using a natural convection solar tunnel dryer. J Food Agric Environ. 2010;8(1):7–12.
[10] Schössler K, Jäger H, Knorr D. Effect of continuous and intermittent ultrasound on drying time and effective diffusivity during convective drying of apple and red bell pepper. J Food Eng. 2012;108(1):103–10.
[11] El-Beltagy A, Gamea GR, Essa AH. Solar drying characteristics of strawberry. J Food Eng. 2007;78(2):456–64.
[12] Akoy EOM. Experimental characterization and modeling of thin-layer drying of mango slices. Int Food Res J. 2014;21(5):1911–7.
[13] Hashim N, Daniel O, Rahaman E. A Preliminary Study: Kinetic model of drying process of Pumpkins (Cucurbita Moschata) in a convective hot air dryer. Agric Agric Sci Proc. 2014;2:345–52.
[14] Omolola AO, Jideani AIO, Kapila PF. Modeling microwave drying kinetics and moisture diffusivity of Mabonde banana variety. Int J Agric Biol Eng. 2014;7(6):107–13.
[15] Ayadi M, Mabrouk SB, Zouari I, Bellagi A. Kinetic study of the convective drying of spearmint. J Saudi Soc Agric Sci. 2014;13(1):1–7.
[16] Kaur K, Singh AK. Drying kinetics and quality characteristics of beetroot slices under hot air followed by microwave finish drying. Afr J Agric Res. 2014;9(12):1036–44.
[17] Demir V, Gunhan T, Yagcioglu AK. Mathematical modelling of convection drying of green table olives. Biosyst Eng. 2007;98(1):47–53.
[18] Sacilik K. Effect of drying methods on thin-layer drying characteristics of hull-less seed pumpkin (Cucurbita pepo L.). J Food Eng. 2007;79:23–30.
[19] Onwude DI, Hashim N, Abdan K, Janius R, Chen G. Experimental studies and mathematical simulation of intermittent infrared and convective drying of sweet potato (Ipomoea batatas L.). Food Bioprod Process. 2019;114:163–74.
[20] Horuz E, Bozkurt H, Karataş H, Maskan M. Drying kinetics of apricot halves in a microwave-hot air hybrid oven. Heat Mass Transf. 2017;53:2117–27.
[21] Arslan D, Özcan MM, Menges HO. Evaluation of drying methods with respect to drying parameters, some nutritional and colour characteristics of peppermint (Mentha x piperita L.). Energy Convers Manag. 2010;51(12):2769–75.
[22] Beigi M. Hot air drying of apple slices: dehydration characteristics and quality assessment. Heat Mass Transf. 2016;52:1435–42.
[23] Salehi F, Kashaninejad M. Effect of drying methods on rheological and textural properties, and color changes of wild sage seed gum. J Food Sci Technol. 2015;52:7361–8.
[24] Maskan M. Kinetics of colour change of kiwifruits during hot air and microwave drying. J Food Eng. 2001;48:169–75.
[25] Tulek Y. Drying kinetic of oyster mushroom (Pleurotus ostreatus) in a convective hot air dryer. J Agric Sci Technol. 2011;13:655–64.
[26] Salehi F, Kashaninejad M, Jafarianlari A. Drying kinetics and characteristics of combined infrared-vacuum drying of button mushroom slices. Heat Mass Transf. 2017;53:1751–9.
[27] Kaleta A, Górnicki K. Evaluation of drying models of apple (var. McIntosh) dried in a convective dryer. Int J Food Sci Technol. 2010;45:891–8.
[28] Olanipekun BF, Tunde-Akintunde TY, Oyelade OJ, Adebisi MG, Adenaya TA. Mathematical modelling of thin-layer pineapple drying. J Food Process & Preservation. 2015;39(6):1431–41.
[29] Therdthai N, Zhou WB. Characterization of microwave vacuum drying and hot air drying of mint leaves (Mentha cordifolia Opiz ex Fresen). J Food Eng. 2009;91:482–9.